Nuclear Engineering and Technology 49 (2017) 776–780

Available online at ScienceDirect

Nuclear Engineering and Technology

journal homepage: www.elsevier.com/locate/net

Original Article

Comparison of Image Uniformity with Photon Counting and Conventional Scintillation Single-Photon Emission Computed Tomography System: A Monte Carlo Simulation Study

Ho Chul Kim [a], *Hee-Joung Kim* [b], *Kyuseok Kim* [b], *Min-Hee Lee* [c], *and Youngjin Lee* [a,*]

[a] *Department of Radiological Science, Eulji University, 553, Sanseong-daero, Seongnam-si, Gyeonggi-do, 13135, South Korea*

[b] *Department of Radiological Science, Yonsei University, 1, Yonseidae-gil, Wonju-si, 26493, South Korea*

[c] *Department of Biomedical Engineering, Yonsei University, 1, Yonseidae-gil, Wonju-si, 26493, South Korea*

ARTICLE INFO

Article history:
Received 3 June 2016
Received in revised form
11 October 2016
Accepted 5 December 2016
Available online 28 December 2016

Keywords:
Medical Application
Monte Carlo Simulation
Nuclear Medicine
Photon Counting Detector
Scintillation Detector
Single-Photon Emission Computed Tomography System

ABSTRACT

To avoid imaging artifacts and interpretation mistakes, an improvement of the uniformity in gamma camera systems is a very important point. We can expect excellent uniformity using cadmium zinc telluride (CZT) photon counting detector (PCD) because of the direct conversion of the gamma rays energy into electrons. In addition, the uniformity performance such as integral uniformity (IU), differential uniformity (DU), scatter fraction (SF), and contrast-to-noise ratio (CNR) varies according to the energy window setting. In this study, we compared a PCD and conventional scintillation detector with respect to the energy windows (5%, 10%, 15%, and 20%) using a ^{99m}Tc gamma source with a Geant4 Application for Tomography Emission simulation tool. The gamma camera systems used in this work are a CZT PCD and NaI(Tl) conventional scintillation detector with a 1-mm thickness. According to the results, although the IU and DU results were improved with the energy window, the SF and CNR results deteriorated with the energy window. In particular, the uniformity for the PCD was higher than that of the conventional scintillation detector in all cases. In conclusion, our results demonstrated that the uniformity of the CZT PCD was higher than that of the conventional scintillation detector.

1. Introduction

Nuclear medicine imaging devices using single-photon emission computed tomography (SPECT) has many advantages in the field of diagnostic medicine or radiotherapy [1–3]. SPECT has become an essential device and is considered a valuable functional imaging tool. In general, to acquire physiological information using SPECT, patients are injected with a suitable

* *Corresponding author.*
E-mail address: radioyoungj@gmail.com (Y. Lee).

http://dx.doi.org/10.1016/j.net.2016.12.002

radioisotope that emits gamma rays. In this technique, the conventional scintillation SPECT system using an NaI(Tl) or CsI(Tl) detector is most frequently used [4–6]. However, a limitation of this system is the inadequate quantitative accuracy of several nonuniformity problems due to difficulties in obtaining a proper energy window setting and scatter radiation [7]. In particular, the common sources of imaging artifacts were nonuniformity in SPECT. To overcome this limitation, a photon counting detector (PCD) using cadmium zinc telluride (CZT) or cadmium telluride (CdTe) has been developed for SPECT [8–10]. Using this, the quantitative accuracy and spectroscopic performance are improved due to the excellent energy resolution and direct conversion of gamma ray energy into electrons [2,4]. Lee and Kim [11] have acquired a high energy resolution (approximately 6.3%) from a 3-mm thick CZT PCD using a ^{57}Co source. The energy resolution of CZT PCD can be seen to be significantly improved when compared with that of a conventional scintillation detector [12].

The frequently used measurement parameters for uniformity are integral uniformity (IU), differential uniformity (DU), scatter fraction (SF), and contrast-to-noise ratio (CNR) [7]. IU and DU are calculated in both useful field of view (UFOV) with a medial region of 95% of FOV and central field of view (CFOV) with a medial region of 75% of UFOV. Fig. 1 shows both UFOV and CFOV descriptions. The standardization level and automation of these parameters are not reached in the field of nuclear medicine imaging. In addition, to the best of our knowledge, only a few studies have performed uniformity tests using a CZT PCD. Thus, herein, we investigated and compared the uniformity performances for different detector materials with respect to the energy window. For this purpose, we evaluated IU, DU, SF, and CNR using the Geant4 Application for Tomographic Emission (GATE) simulation (developed by International OpenGATE collaboration).

2. Materials and methods

2.1. Simulation set up

Simulation tools of the gamma camera or SPECT imaging are applicable in the field of nuclear medicine [13–15]. These tools are useful in assessing imaging characteristics and quantitative accuracy [16]. In this study, among various simulation tools, we used the GATE simulation tool, which is very powerful and widely used in the field of nuclear medicine, and which is based on the Monte Carlo platform. We simulated SPECT using CZT PCDs and conventional NaI(Tl) scintillation detectors. The geometries of and information on these detectors are presented in Table 1. In consideration of the intrinsic resolution, we separately designed the size and number of pixels. Moreover, charge sharing was not simulated due to the clear and acceptable image quality of the CZT PCD.

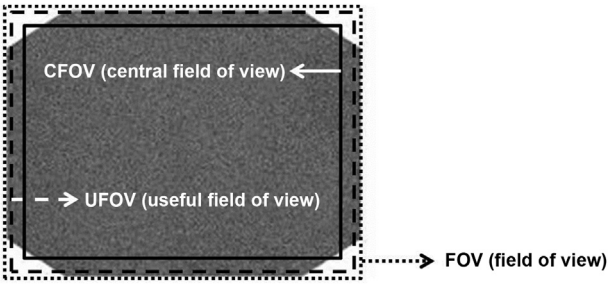

Fig. 1 – Schematic description of field of view (FOV), central field of view (CFOV), and useful field of view (UFOV).

2.2. Evaluation of image uniformity

To evaluate image uniformity, we calculated IU, DU, SF, and CNR. We simulated a ^{99m}Tc (140 keV energy peak) point source with an activity of 1 MBq and used a 900-second scan time to evaluate IU and DU. In addition, we designed a hot-rod phantom using GATE with different diameters to estimate SF and CNR (Fig. 2). The number of projections was 90 over 360 degrees (acquisition time of 1 view: 10 seconds); image reconstruction was carried out using an ordered subset-expectation maximization method with five iterations and five subsets. The 5%, 10%, 15%, and 20% symmetrical energy windows were applied. Table 2 shows the range of the energy window for each detector system.

The values of IU and DU were calculated as follows [7]:

$$\mathrm{IU}(\%) = 100 \times \frac{M_{\mathrm{pixel}} - m_{\mathrm{pixel}}}{M_{\mathrm{pixel}} + m_{\mathrm{pixel}}} \quad (1)$$

$$\mathrm{DU}(\%) = 100 \times \frac{M_{\mathrm{local}} - m_{\mathrm{local}}}{M_{\mathrm{local}} + m_{\mathrm{local}}} \quad (2)$$

where M_{pixel} is the maximum pixel count, m_{pixel} is the minimum pixel count, M_{local} is the maximum percentage pixel count for all rows and columns in a localized line of pixels, and m_{local} is the maximum percentage pixel count for all rows and columns in a localized line of pixels.

The values of SF and CNR, which indicate the value of energy distortion, were calculated as follows [12, 17]:

$$\mathrm{SF}(\%) = 100 \times \frac{P_{\mathrm{scattered}}}{P_{\mathrm{primary}} + P_{\mathrm{scattered}}} \quad (3)$$

$$\mathrm{CNR} = \frac{\left|P_{\mathrm{ROI.rod}} - P_{\mathrm{ROI.background}}\right|}{\sqrt{\sigma^2_{\mathrm{ROI.rod}} + \sigma^2_{\mathrm{ROI.background}}}} \quad (4)$$

where $P_{\mathrm{scattered}}$ is the number of scattered gamma rays, P_{primary} is the number of primary gamma rays, $P_{\mathrm{ROI.rod}}$ is the count of hot-rod regions in the phantom, $P_{\mathrm{ROI.background}}$ is the count of background regions in the phantom, and $\sigma_{\mathrm{ROI.rod}}$ and $\sigma_{\mathrm{ROI.background}}$ are the standard deviation of the hot-rod region and the background in the phantom, respectively.

Table 1 – Specifications of two detector materials for evaluation of image uniformity.

Materials	CZT	NaI(Tl) scintillator
Thickness (mm)	1	1
Detector size (mm^2)	44.8 × 44.8	44.8 × 44.8
Pixel size (mm^2)	0.35 × 0.35	1.4 × 1.4
No. of pixels	128 × 128	32 × 32
Energy resolution (%)	6	9

CZT, cadmium zinc telluride.

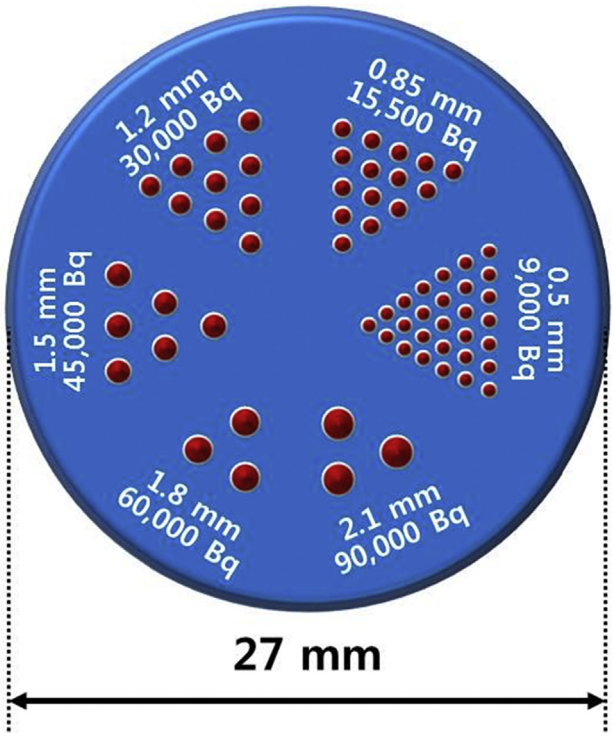

Fig. 2 – Hot-rod phantom diagram. The phantom consisted of six areas with rods of varying diameters (0.5 mm, 0.85 mm, 1.2 mm, 1.5 mm, 1.8 mm, and 2.1 mm) that can be filled with activity. Activities were 9 kBq, 15.5 kBq, 30 kBq, 45 kBq, 60 kBq, and 90 kBq, respectively.

Ten sets of simulation results were acquired for each detector system; error range (σ_{error}) was calculated as follows:

$$\sigma_{error} = \sqrt{\frac{\sum_{i=1}^{n}(N_i - \overline{N})^2}{(n-1)}} \quad (5)$$

where n is the number of measurements taken ($n = 10$), N_i is the datum from each measurement, and $\overline{N}$ is the measured average of the data.

Table 2 – Specifications of eight detector systems with different energy windows.

Detector system	Energy window (%)	Energy range (symmetrical) (keV)
CZT-1	5	136.5–143.5
CZT-2	10	133–147
CZT-3	15	129.5–150.5
CZT-4	20	126–154
NaI(Tl)-1	5	136.5–143.5
NaI(Tl)-2	10	133–147
NaI(Tl)-3	15	129.5–150.5
NaI(Tl)-4	20	126–154

CZT, cadmium zinc telluride.

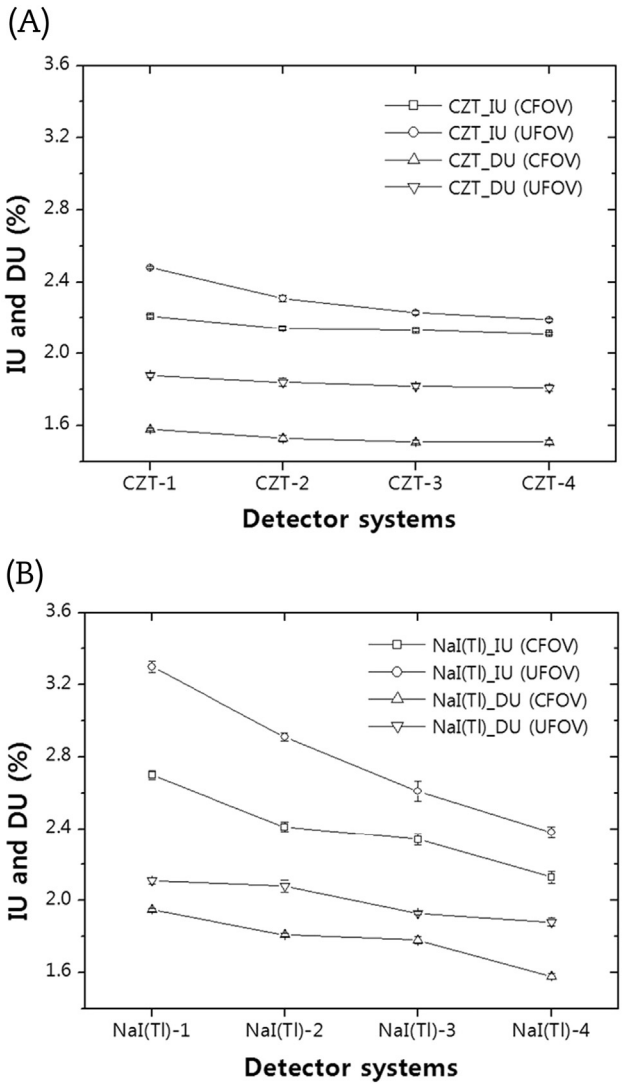

Fig. 3 – Plot of the IU and DU in UFOV and CFOV. (A) With CZT detector systems and (B) with NaI(Tl) detector systems. CFOV, central field of view; CZT, cadmium zinc telluride; DU, differential uniformity; IU, integral uniformity; UFOV, useful field of view.

3. Results and discussion

One of the main defects in the SPECT system is its relatively low image uniformity. The uniformity is affected by a scatter radiation due to spectral distortion in the energy spectrum. Therefore, in the field of nuclear medicine, the scatter rejection method is very important for the improvement in uniformity. The conventional scintillation detectors using NaI(Tl) material are generally used in this field, but these detectors have a limitation of lower energy resolution. To cope with this problem, a PCD using CZT material has been developed that efficiently generates electrons and holes. In our previous study, the measured energy resolution of a CZT PCD (eValuator-2500; eV Products, Arizona, USA) was approximately 6.3% full width at half maximum [11]. Compared with the spectra obtained on a conventional scintillation detector, one can notice a markedly better energy resolution with CZT PCD [the

energy resolution of NaI(Tl) scintillation detector can be acquired by approximately 10% full width at half maximum] [18, 19].

The uniformity can be divided into two types: (1) intrinsic uniformity and (2) system uniformity. The intrinsic uniformity is generally measured using ^{99m}Tc source with smoothing filter and is calculated by IU and DU in both UFOV and CFOV. Moreover, as aforementioned, the scatter radiation and energy window setting affect image uniformity. The purpose of this study was to evaluate and compare the uniformities with CZT PCD and NaI(Tl) scintillation detectors using a calculated IU, DU, SF, and CNR.

The evaluated IU and DU in UFOV and CFOV for each detector system are shown in Fig. 3 and Table 3. The results from IU and DU demonstrate that the CZT-1, CZT-2, CZT-3, and CZT-4 detector systems were lower than NaI(Tl)-1, NaI(Tl)-2, NaI(Tl)-3, and NaI(Tl)-4 detector systems, respectively (for the same detector thickness and energy window conditions). In particular, we compared the CZT-4 detector system with an NaI(Tl)-4 detector system that had been demonstrated to have a 1.27-times higher average of IU and a 1.17-times higher average of DU (for 1 mm and 20% energy window conditions).

In addition, the evaluated IU and DU results go from 5%, via 10% and 15%, to the 20% energy window in increasing order for all cases (Fig. 3). In CZT PCDs, the average IU in UFOV and CFOV using a 20% energy window was 1.01 times, 1.03 times, and 1.09 times better than those obtained with 15%, 10%, and 5% energy windows, respectively; and in the NaI(Tl) detector systems, the average IU in UFOV and CFOV using 20% energy window was 1.09 times, 1.18 times, and 1.33 times better than those obtained with 15%, 10%, and 5% energy windows, respectively. Moreover, in CZT PCDs, the average IU in UFOV and CFOV using a 20% energy window was 1.01 times, 1.02 times, and 1.04 times better than that obtained with 15%, 10%, and 5% energy windows, respectively; in the NaI(Tl) detector systems, the average IU in UFOV and CFOV using a 20% energy window was 1.07 times, 1.12 times, and 1.17 times better than those obtained with 15%, 10%, and 5% energy windows, respectively.

The evaluated SF and CNR for each detector system are shown in Figs. 4 and 5, and Table 4. The results from SF and CNR demonstrate that the CZT-1, CZT-2, CZT-3, and CZT-4 detector systems were better than the NaI(Tl)-1, NaI(Tl)-2, NaI(Tl)-3, and NaI(Tl)-4 detector systems, respectively (for identical detector thickness and energy window conditions). We compared the CZT-1 detector system with the NaI(Tl)-1 detector system, which had been demonstrated to have a 1.33 times lower average of SF and a 1.21 times higher average of CNR (for 1 mm and 5% energy window conditions).

In CZT PCDs, the average SF when using a 5% energy window was 1.05 times, 1.11 times, and 1.22 times better than those obtained with 10%, 15%, and 20% energy windows, respectively; and in the NaI(Tl) detector systems, the average CNR when using a 5% energy window was 1.03 times, 1.04 times, and 1.09 times higher than those obtained with 10%, 15%, and 20% energy windows, respectively. Moreover, in CZT PCDs, the average SF when using a 5% energy window was 1.05 times, 1.11 times, and 1.23 times better than those obtained with 10%, 15%, and 20% energy windows, respectively; in the NaI(Tl) detector systems, the average CNR using a 5% energy window was 1.04 times, 1.10 times, and 1.15 times

Table 3 – IU and DU in UFOV and CFOV with respect to the detector systems.

Detector system	IU (%, UFOV)	IU (%, CFOV)	DU (%, UFOV)	DU (%, CFOV)
CZT-1	2.48	2.21	1.88	1.58
CZT-2	2.31	2.48	1.84	1.53
CZT-3	2.23	2.13	1.82	1.51
CZT-4	2.19	2.11	1.81	1.51
NaI(Tl)-1	3.30	2.70	2.11	1.95
NaI(Tl)-2	2.91	2.41	2.08	1.81
NaI(Tl)-3	2.61	2.34	1.93	1.78
NaI(Tl)-4	2.38	2.31	1.88	1.58

CFOV, central field of view; CZT, cadmium zinc telluride; DU, differential uniformity; IU, integral uniformity; UFOV, useful field of view.

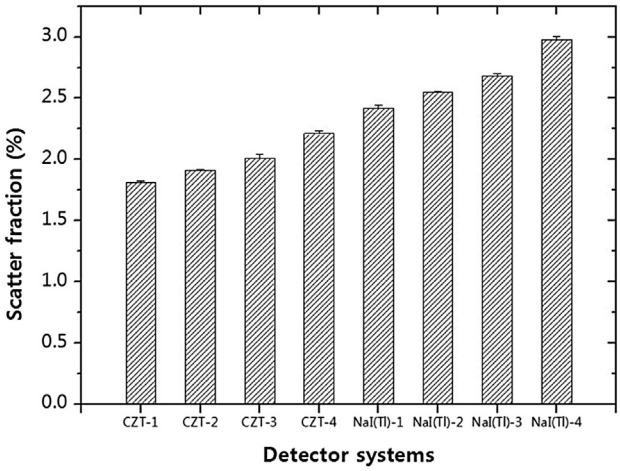

Fig. 4 – Plot of scatter fraction with respect to the detector system. CZT, cadmium zinc telluride.

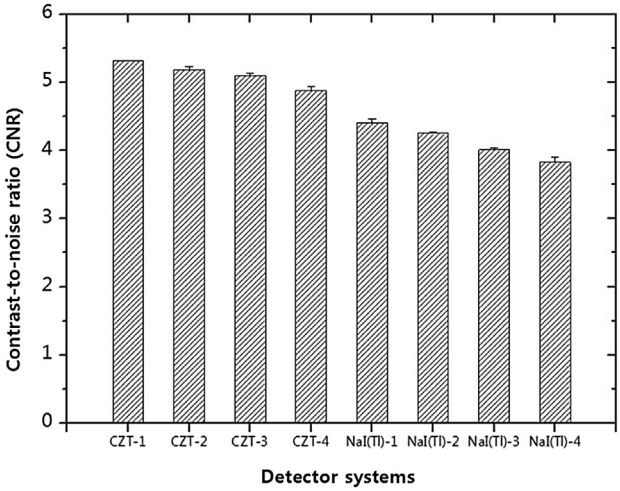

Fig. 5 – Plot of contrast-to-noise ratio with respect to the detector system. CZT, cadmium zinc telluride.

Table 4 – SF and CNR with respect to the detector systems.

Detector system	SF (%)	CNR
CZT-1	1.81	5.31
CZT-2	1.91	5.18
CZT-3	2.01	5.10
CZT-4	2.21	4.88
NaI(Tl)-1	2.41	4.40
NaI(Tl)-2	2.55	4.25
NaI(Tl)-3	2.68	4.01
NaI(Tl)-4	2.98	3.83

CNR, contrast-to-noise ratio; CZT, cadmium zinc telluride; SF, scatter fraction.

higher than those obtained with 10%, 15%, and 20% energy windows, respectively.

In accordance with these results, we can improve the uniformity using CZT PCD. In addition, although the 20% energy window is generally used in the field of nuclear medicine, as suggested by this study, the efficient energy window is different. For a wider energy window, there was no clear change in the evaluated data of IU and DU in UFOV and CFOV to indicate the optimal energy window setting. In addition, for the narrower energy window, there was no clear change in the evaluated data of SF and CNR to indicate the optimal energy window setting.

4. Conclusion

Because the measurement of uniformity is performed on a daily basis, it is very important to maintain the gamma camera system. We have presented comparable results of uniformity for different detector systems. Our results show that the effect of detector material and energy window setting can be investigated. Based on the results, CZT PCD produced better uniformity at all energy windows.

Conflicts of interest

The authors have no conflicts of interest to declare.

REFERENCES

[1] R.J. Jaszczak, R.E. Goleman, C.B. Lim, SPECT: single photon emission computed tomography, IEEE Trans. Nucl. Sci. NS-27 (1980) 1137–1153.

[2] Y.J. Lee, H.J. Ryu, S.W. Lee, S.J. Park, H.J. Kim, Comparison of ultra-high-resolution parallel-hole collimator materials based on the CdTe pixelated semiconductor SPECT system, Nucl. Instrum. Methods Phys. Res. A 713 (2013) 33–39.

[3] M.T. Madsen, Recent advances in SPECT imaging, J. Nucl. Med. 48 (2007) 661–673.

[4] Y.-J. Lee, S.-J. Park, D.-H. Kim, H.-J. Kim, Optimization of the SPECT systems based on a CdTe pixelated semiconductor detector using novel parallel-hole collimators, J. Instrum. 9 (2014) C05057.

[5] C.L. Melcher, J.S. Schweitzer, R.A. Manente, C.A. Peterson, Applications of single crystals in oil well logging, J. Cryst. Growth 109 (1991) 37–42.

[6] T.E. Peterson, L.R. Furenlid, SPECT detectors: the Anger Camera and beyond, Phys. Med. Biol. 7 (2011) R145–R182.

[7] M.A.K. Abdelhalim, R.A.-M. Rizk, H.I. Farag, S.M. Reda, Effect of energy window width on planer and SPECT image uniformity, J. King Saud Univ. 21 (2009) 145–150.

[8] C. Scheiber, CdTe and CdZnTe detectors in nuclear medicine, Nucl. Instrum. Methods Phys. Res. A 448 (2000) 513–524.

[9] A. Abe, N. Takahashi, J. Lee, T. Oka, K. Shizukuishi, T. Kikuchi, T. Inoue, M. Jimbo, H. Ryuo, C. Bickel, Performance evaluation of a hand-held, semiconductor (CdZnTe)-based gamma camera, Eur. J. Nucl. Med. Mol. Imaging 30 (2003) 805–811.

[10] K. Ogawa, M. Muraishi, Feasibility study on an ultra-high-resolution SPECT with CdTe detectors, IEEE Trans. Nucl. Sci. 57 (2010) 17–24.

[11] Y. Lee, H.-J. Kim, Performance evaluation of a small CZT pixelated semiconductor gamma camera system with a newly designed stack-up parallel-hole collimator, Nucl. Instrum. Methods Phys. Res. A 794 (2015) 54–61.

[12] T. Onodera, K. Hitomi, T. Shoji, Y. Hiratate, Pixellated thallium bromide detectors for gamma-ray spectroscopy and imaging, Nucl. Instrum. Methods Phys. Res. A 525 (2004) 199–204.

[13] A. Konik, M.T. Madsen, J.J. Sunderland, GATE simulations of small animal SPECT for determination of scatter fraction as a function of object size, IEEE Trans. Nucl. Sci. 59 (2012) 1887–1891.

[14] S. Stute, T. Carlier, K. Cristina, C. Noblet, A. Martineau, B. Hutton, L. Barnden, I. Buvat, Monte Carlo simulations of clinical PET and SPECT scans: impact of the input data on the simulated images, Phys. Med. Biol. 56 (2011) 6441–6457.

[15] J.S. Fleming, Evaluation of a technique for simulation of gamma camera images, Phys. Med. Biol. 41 (1996) 1855–1861.

[16] S. Jan, D. Benoit, E. Becheva, T. Carlier, F. Cassol, P. Descourt, T. Frisson, L. Grevillot, L. Guigues, L. Maigne, C. Morel, Y. Perrot, N. Rehfeld, D. Sarrut, D.R. Schaart, S. Stute, U. Pietrzyk, D. Visvikis, N. Zahra, I. Buvat, GATE V6: a major enhancement of the GATE simulation platform enabling modelling of CT and radiotherapy, Phys. Med. Biol. 56 (2011) 881–901.

[17] P.-H. Jeon, C.-L. Lee, D.-H. Kim, Y.-J. Lee, S.-S. Jeon, H.-J. Kim, Dose reduction and image quality optimizations in CT of pediatric and adult patients: phantom studies, J. Instrum. 9 (2014) P03013.

[18] J.-H. Kim, Y. Choi, K.-S. Joo, B.-S. Sihn, J.-W. Chong, S.E. Kim, K.H. Lee, Y.S. Choe, B.-T. Kim, Development of a miniature scintillation camera using an NaI(Tl) scintillator and PSPMT for scintimammography, Phys. Med. Biol. 45 (2000) 3481–3488.

[19] M. Moszynski, J. Zalipska, M. Balcerzyk, M. Kapusta, W. Mengesha, J.D. Valentine, Intrinsic energy resolution of NaI(Tl), Nucl. Instrum. Methods Phys. Res. A 484 (2002) 259–269.